MODELING, ANALYSIS AND CONTROL OF STATIC VAR COMPENSATOR USING THREE-LEVEL INVERTER

Guk C. Cho(*), *Nam S. Choi*(*), *Chun T. Rim*(**) *and Gyu H. Cho*(*)

(*) Dept. of Electrical Engineering,
Korea Advanced Institute of Science and Technology (KAIST),
373-1, Kusong Dong, Yusong Gu, Taejon, 305-701, Korea (FAX : 82-42-869-3410)
(**) Dept. of R & D, Defence Communication Research Agency,
Seoul P.O.Box 932, 100-609, Seoul, Korea (FAX : 82-42-756-1383)

Abstract: *A new static var compensator(SVC) system using three-level inverter is proposed for high voltage and high power applications. A general and simple model for the overall system is obtained using circuit DQ-transform and DC and AC analyses are achieved to characterize the open-loop system. Using the proposed model, a new control method which controls both the phase angle and modulation index of switching pattern simultaneously is suggested to provide fast response of SVC system without using independent voltage source. Finally, predicted results are verified by computer simulation.*

I. INTRODUCTION

The advantages of introducing force-commutated inverters and rectifiers in reactive power compensation have been confirmed by many researchers and are gradually being recognized by the static converter industry and the large-scale users of electric power. These advantages include the cost reduction of the associated reactive components, precise and continuous reactive power control and reduced potential size and weight[1][2]. So far, SVC's using two-level inverter have been proposed as shown in Fig. 1[3]-[6]. Due to the rating restriction of the switching devices in the inverter, it is difficult to apply SVC using two-level inverter for high voltage and high power applications[7].

To overcome this disadvantage, SVC system using three-level inverter instead of two-level inverter is chosen as shown in Fig. 2 in this paper, because three-level inverter has lower voltage stress and lower harmonic components and can be operated at lower switching frequency[7]. A general and simple model for the proposed SVC system is derived by using the circuit DQ-transform[8] and DC and AC analyses are done to reveal the behavior of the open-loop system. In addition, a new control method which controls the phase angle(α) and modulation index(MI) of switching pattern simultaneously to achieve fast dynamic response of SVC system with self-controlled dc capacitor without using independent voltage source. Predicted results are shown by computer simulation.

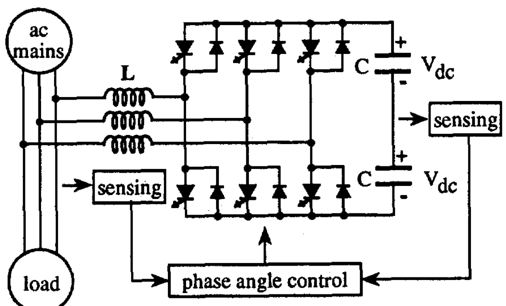

(a)

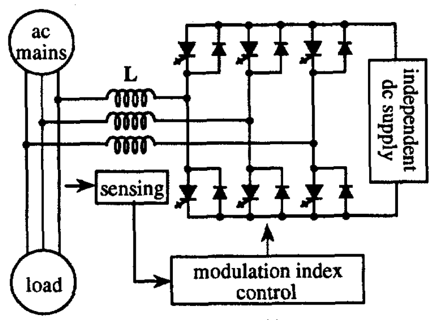

(b)

Fig. 1 SVC using two-level inverter

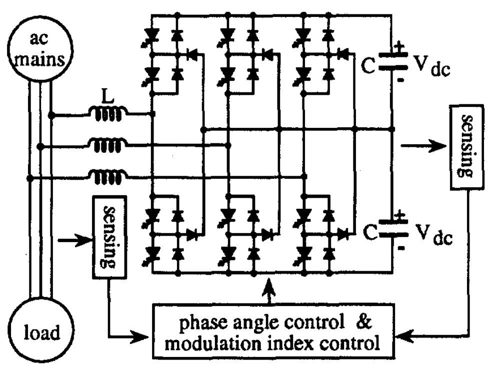

Fig. 2. SVC using three-level inverter

0-7803-0634-1/92$03.00 ©IEEE

II. PRINCIPLE OF OPERATION

The operating principle of the SVC system can be explained by considering a voltage source connected to the ac mains through a reactor and a resistor representing the total loss in the inverter as shown in Fig. 3. Fig. 3(b) shows the phasor diagram for leading power factor and Fig. 3(c) for lagging power factor. By controlling the phase angle(α) of switching pattern, the independent voltage source shown in Fig. 1(b) can be omitted[3]. Fast dynamic response of SVC irrespective of capacitor in the inverter can be achieved by controlling the modulation index(MI) of switching pattern simultaneously. More detailed operation is described by analyzing the equivalent circuit obtained in later section.

III. MODELING

The main circuit of SVC shown in Fig. 4 is modeled in this section. Equivalent circuit is obtained by circuit DQ-transform method with the following assumptions:

i) all switches are ideal,
ii) the source voltages are balanced,
iii) line impedance and total loss of the inverter is represented by lumped resistor R_s,
iv) harmonic components generated by switching action are negligible.

The original system is too complex to analyze. So it is partitioned to several basic sub-circuits. There are five basic sub-circuits in this switching system. They are voltage source set, resistor set, inductor set, switch set and DC circuit.

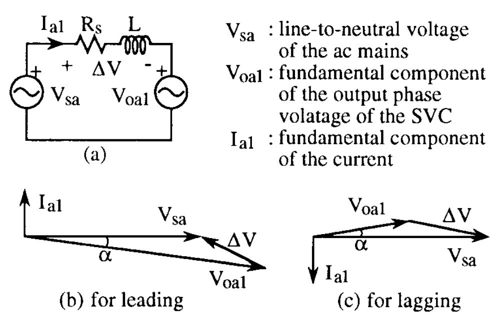

Fig. 3 single-phase equivalent circuit

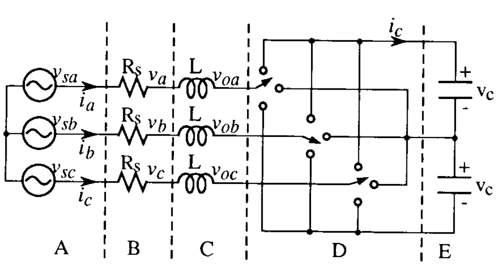

Fig. 4. main circuit of SVC

The rotationary three-phase circuits are now transformed to stationary circuits. The time-varying nature of the switching system is eliminated in this way. The voltage source and power invariant DQ-transform matrix are given as follows:

$$\mathbf{v}_{s,abc} = \begin{bmatrix} v_{sa} \\ v_{sb} \\ v_{sc} \end{bmatrix} = \sqrt{2/3}\ V_s \begin{bmatrix} \sin\omega t \\ \sin(\omega t - 2\pi/3) \\ \sin(\omega t + 2\pi/3) \end{bmatrix}, \qquad (1)$$

$$\mathbf{K} = \sqrt{2/3} \begin{bmatrix} \cos(\omega t+\alpha) & \cos(\omega t+\alpha-2\pi/3) & \cos(\omega t+\alpha+2\pi/3) \\ \sin(\omega t+\alpha) & \sin(\omega t+\alpha-2\pi/3) & \sin(\omega t+\alpha+2\pi/3) \\ 1/\sqrt{2} & 1/\sqrt{2} & 1/\sqrt{2} \end{bmatrix},$$

$$\mathbf{K}^{-1} = \mathbf{K}^T \qquad (2)$$

where

$$\mathbf{x}_{qdo} = \mathbf{K}\,\mathbf{x}_{abc} \ . \qquad (3)$$

A. Transform of Part A, B

The voltage and current relation about resistor R_s is

$$\mathbf{v}_{s,abc} = R_s \mathbf{i}_{abc} + \mathbf{v}_{abc} \ , \qquad (4)$$

and the circuit DQ-transformed result becomes

$$\mathbf{v}_{s,qdo} = R_s \mathbf{i}_{qdo} + \mathbf{v}_{qdo} \qquad (5)$$

where

$$\mathbf{v}_{s,qdo} = \mathbf{K}\mathbf{v}_{s,abc} = V_s \begin{bmatrix} -\sin\alpha \\ \cos\alpha \\ 0 \end{bmatrix}. \qquad (6)$$

From (5) the equivalent circuit of part A, B is obtained as shown in Fig. 5(a).

B. Transform of Part C

The voltage and current relation about inductor L is

$$L\dot{\mathbf{i}}_{abc} = \mathbf{v}_{abc} - \mathbf{v}_{o,abc} \qquad (7)$$

and the circuit DQ-transformed result becomes

$$L\dot{\mathbf{i}}_{qdo} = L\dot{\mathbf{K}}\mathbf{K}^{-1}\mathbf{i}_{qdo} + \mathbf{v}_{qdo} - \mathbf{v}_{o,qdo} \ . \qquad (8)$$

That is,

$$L\dot{i}_q = -\omega L i_d + v_q - v_{oq} \qquad (9)$$

$$L\dot{i}_d = \omega L i_q + v_d - v_{od} \ . \qquad (10)$$

From (9) and (10) the inductor set becomes a second order gyrator-coupled system as shown in Fig. 5(b).

C. Transform of Part D, E

Under the assumption that harmonic components generated by switching action in inverter are negligible, switching function S can be defined as follows:

$$\mathbf{S} = \begin{bmatrix} S_a \\ S_b \\ S_c \end{bmatrix} = \sqrt{2/3}\, d \begin{bmatrix} \sin(\omega t + \alpha) \\ \sin(\omega t + \alpha - 2\pi/3) \\ \sin(\omega t + \alpha + 2\pi/3) \end{bmatrix}. \quad (11)$$

Phase angle α is the phase difference between source voltage and switching function. Using the switching function **S** the output voltage of inverter can be represented as below:

$$\mathbf{v}_{o,abc} = \mathbf{S} v_c \quad (12)$$

and by using circuit DQ-transform of (10) $v_{o,qdo}$ is given by

$$\mathbf{v}_{o,qdo} = \mathbf{K}\mathbf{S} v_c = \begin{bmatrix} 0 \\ d \\ 0 \end{bmatrix} v_c \ . \quad (13)$$

Note that modulation index is given by

$$MI = v_{oa,peak}/v_c = \sqrt{2/3}d \ . \quad (14)$$

Using the switching function **S**, the capacitor dc current is represented by

$$2i_c = \mathbf{S}^T \mathbf{i}_{abc} = \mathbf{S}^T \mathbf{K}^{-1} i_{qdo} = \begin{bmatrix} 0 & d & 0 \end{bmatrix} \begin{bmatrix} i_q \\ i_d \\ i_o \end{bmatrix}. \quad (15)$$

From (13), (15) the switch set becomes transformer as shown in Fig. 5(c).

The method of circuit reconstruction for the sub-circuits obtained above is to connect adjacent related parts where the voltage and current are in common. The result is shown in Fig. 6. This circuit can be directly used in finding DC operating point and in analyzing the dynamic characteristics of SVC system.

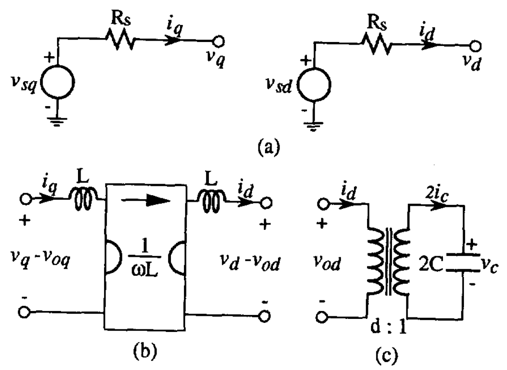

Fig. 5. DQ-transform of sub-circuits

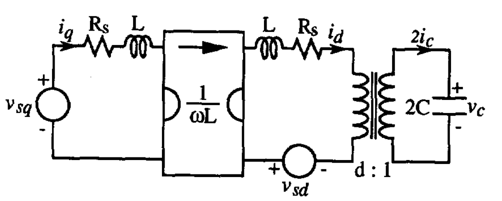

Fig. 6. the equivalent circuit

IV. ANALYSIS

About the equivalent circuit obtained in the previous chapter dc analysis is done to find the operating point and ac analysis is achieved to find the transient characteristics of the SVC system.

A. DC Analysis

The DC analysis can be done the steady-state circuit as shown in Fig. 7 obtained from Fig. 6 by shorting the inductors and opening the capacitor. For given α and D, we obtain

$$V_c = \frac{1}{D}\left(V_{sd} + \frac{\omega L}{R_s} V_{sq}\right), \quad (16)$$

$$I_q = \frac{V_{sq}}{R_s}, \quad I_d = 0 \quad (17)$$

where $V_{sq} = -V_s \sin\alpha$, $V_{sd} = V_s \cos\alpha$.

By the inverse circuit DQ-transform, the line current of a-phase is given by

$$i_a(t) = \sqrt{2/3} I_q \cos\omega t \ . \quad (18)$$

For the system parameters given by

$$L = 5\,\text{mH},\ R_s = 1\,\Omega,\ C = 2000\,\mu\text{F},\ V_s = 220\,V \quad (19)$$

and the control variables given by

$$\alpha = -5^o,\ D = (0.8\sqrt{3/2}) \quad (20)$$

the theoretical results by (16), (17) and (18) from the dc equivalent circuit are as follows:

$V_{sq} = 19\,[V]$ $V_{sd} = 219\,[V]$ $V_c = 260\,[V]$
$I_q = 19\,[A]$ $I_d = 0\,[A]$ $I_{a,peak} = 16\,[A]$

The selected theoretical results are verified by the simulation results of the original circuit. Simulation results are shown in Fig. 8. As shown above, the operating point is determined by the phase angle(α) and the modulation index(MI) of the switching pattern.

B. AC Analysis

To know the dynamic characteristics of SVC system, the small signal analysis is to be done. For a given operating point, small signal equivalent circuit is derived based on the following assumptions:

i) the second order terms (products of variations) are negligible,

ii) the phase angle(α) of switching pattern is small.

With the above assumptions we can obtain

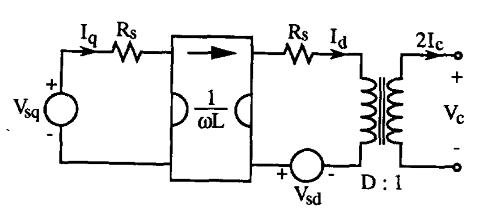

Fig. 7. the equivalent circuit for DC

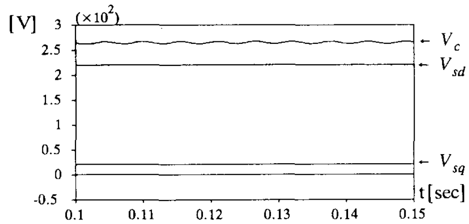

(a) the voltages of V_c, V_{sd} and V_{sq}

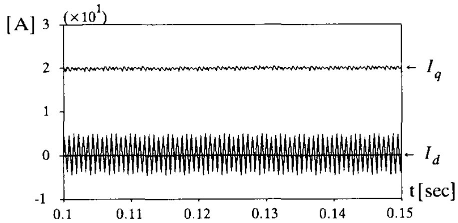

(b) the currents of I_q and I_d

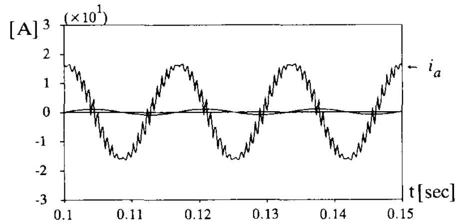

(c) the current of i_a

Fig. 8. simulation of the original circuit for DC

$$v_{od}(t)=d(t)v_c(t)=(D+\hat{d})(V_c+\hat{v}_c)$$
$$\approx D\,V_c+D\,\hat{v}_c+\hat{d}\,V_c \tag{21}$$
$$2i_c(t)=d(t)i_d(t)=(D+\hat{d})\hat{i}_d\approx D\,\hat{i}_d \tag{22}$$
$$\sin\alpha\approx\alpha\,,\quad \cos\alpha\approx 1\,. \tag{23}$$

By using (21), (22) and (23), small signal equivalent circuit is derived as shown in Fig. 9 from Fig. 6.

Applying Laplace transform, the final equations for the system are given by

$$\begin{bmatrix} Ls+R_s & \omega L & 0 \\ -\omega L & Ls+R_s & D \\ 0 & -D & 2Cs \end{bmatrix}\begin{bmatrix} \hat{i}_q(s) \\ \hat{i}_d(s) \\ \hat{v}_c(s) \end{bmatrix}=\begin{bmatrix} -V_s\hat{\alpha}(s) \\ -V_c\hat{d}(s) \\ 0 \end{bmatrix}. \tag{24}$$

Therefore, we can write

$$\begin{bmatrix} \hat{i}_q(s) \\ \hat{i}_d(s) \\ \hat{v}_c(s) \end{bmatrix}=\frac{1}{A(s)}\begin{bmatrix} 2(Ls+R_s)Cs+D^2 & -2\omega LCs & D\,\omega L \\ 2\omega LCs & 2(Ls+R_s)Cs & -D\,(Ls+R_s) \\ D\,\omega L & D\,(Ls+R_s) & (Ls+R_s)^2+(\omega L)^2 \end{bmatrix}\begin{bmatrix} -V_s\,\hat{\alpha}(s) \\ -V_c\,\hat{d}(s) \\ 0 \end{bmatrix} \tag{25}$$

where $A(s)=2CL^2s^3+4LCR_s s^2+[\,2C\,\{R_s^{\,2}+(\omega L)^2\}+D^2L\,]\,s+D^2R_s$.

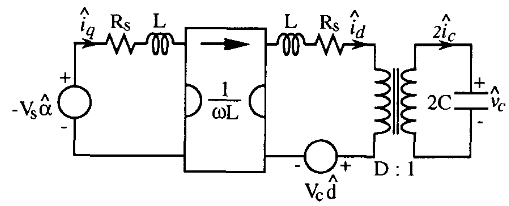

Fig. 9. the equivalent circuit for small signal

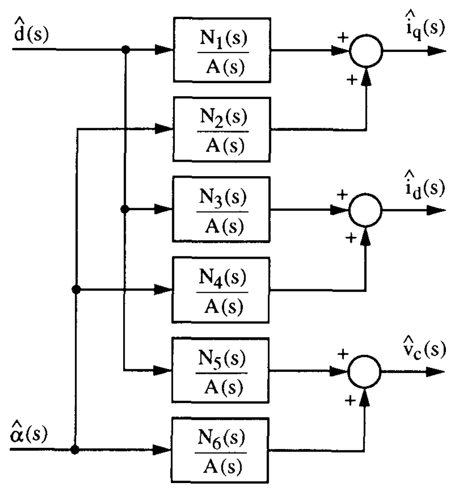

Fig. 10. block diagram for small signal

From (25), the block diagram of the open-loop SVC system for small signal is obtained as shown in Fig. 10.

$$N_1(s)\;=\;2V_c\omega LCs \tag{26a}$$
$$N_2(s)\;=\;-V_s\,(2LCs^2+2R_sCs+D^2) \tag{26b}$$
$$N_3(s)\;=\;-2V_cC\,(Ls+R_s)s \tag{26c}$$
$$N_4(s)\;=\;-2V_s\omega LCs \tag{26d}$$
$$N_5(s)\;=\;-DV_c(Ls+R_s) \tag{26e}$$
$$N_6(s)\;=\;-DV_s\omega L \tag{26f}$$

From (25), the important transfer functions of the SVC system are given as follows:

$$\frac{\hat{v}_c(s)}{\hat{d}(s)}=-\frac{DV_c(Ls+R_s)}{A(s)} \tag{27a}$$
$$\frac{\hat{v}_c(s)}{\hat{\alpha}(s)}=-\frac{DV_s\omega L}{A(s)} \tag{27b}$$

$$\frac{\hat{i}_q(s)}{\hat{d}(s)} = \frac{2V_c \omega LCs}{A(s)} . \tag{28}$$

To check the validity of proposed analysis, the step responses of (27) and (28) using MATLAB are compared with the step responses of the original circuit of the SVC system under the system parameters given by (19) with the control variables

$$\alpha = 0^o \ , \quad D = (0.8\sqrt{3/2}) \ . \tag{29}$$

Fig. 11 and 12 show the step responses of $\hat{v}_c$ for step input $\hat{d}(t) = 0.1\,u(t)$ and for step input $\hat{\alpha}(t) = -5\,u(t)[deg.]$, respectively. Fig. 13 shows the step response of $\hat{i}_q(s)$ for step input $\hat{d}(t) = 0.1\,u(t)$.

As shown above, the close agreement between the analytical and simulational results proves the validity of the modeling and analysis.

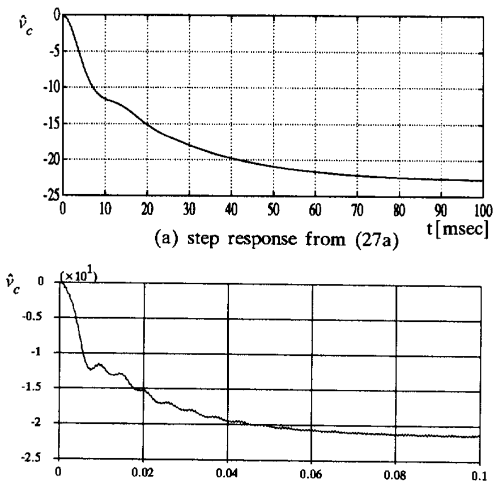

Fig. 11. step response of $\hat{v}_c$ for input $\hat{d}$

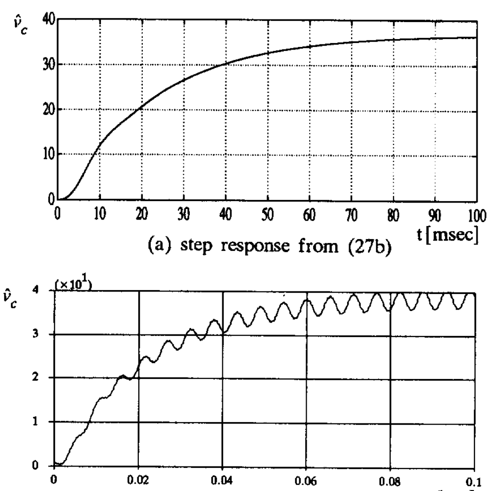

Fig. 12. step response of $\hat{v}_c$ for input $\hat{\alpha}$

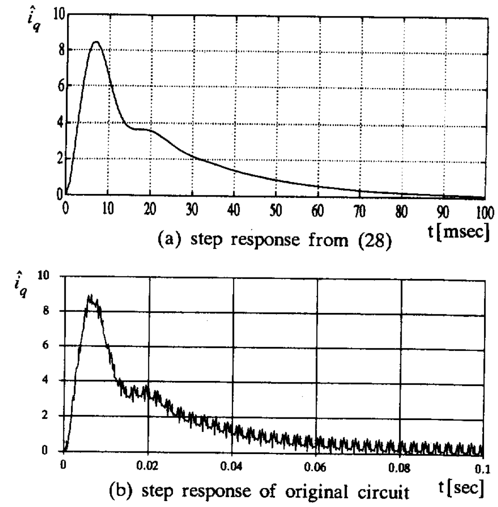

Fig. 13. step response of $\hat{i}_q$ for input $\hat{d}$

V. CONTROLLER DESIGN

To achieve fast dynamic response without using independent DC voltage source, as shown in Fig. 2, it is required that the capacitor voltage v_c should be kept constant by controlling the phase angle(α) while compensating the load reactive power by controlling the modulation index of switching function simultaneously. From (27) $\hat{v}_c(s)$ is given by

$$\hat{v}_c(s) = -\frac{DV_c(Ls+R_s)\hat{d}(s) + DV_s\omega L\,\hat{\alpha}(s)}{A(s)} . \tag{30}$$

In order to make the capacitor voltage constant, the numerator of right-hand side of (30) must be zero. Therefore,

$$\hat{\alpha}(s) = -\frac{V_c(Ls+R_s)}{V_s\omega L}\hat{d}(s) . \tag{31}$$

The authors propose the PI and feedforward control methods which are shown as follows:

i) phase angle(α) control for keeping constant capacitor voltage:

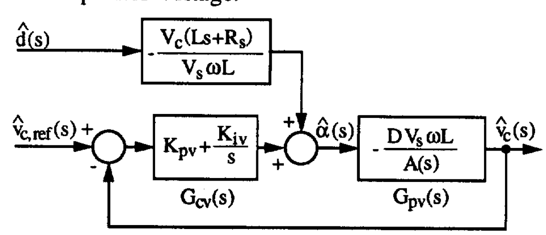

ii) modulation index(MI) control for compensating load vars simultaneously:

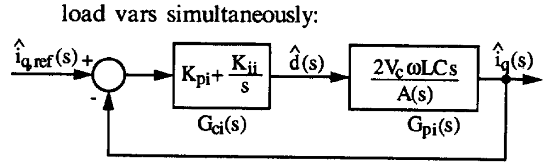

The parameters K_{pv}, K_{iv}, K_{pi} and K_{ii} can be determined by using root-locus technique.

VI. SIMULATION RESULTS

To check the validity of the proposed control method, computer simulation is done using the system parameters given by

$$L = 5\,\text{mH} \quad R_s = 1\,\Omega \quad C = 2000\,\mu\text{F} \quad V_s = 220\,V$$

with the control parameters given by

$$K_{pv} = -7\times10^{-3}, \quad K_{iv} = -0.45$$
$$K_{pi} = 1\times10^{-4}, \quad K_{ii} = 0.95 .$$

By the proposed control method, the capacitor voltage is fixed as follows:

$$v_c = 224.5\,V .$$

Fig. 14 and 15 show the transient response of the total SVC system for a step change in the load power factor. The load power factor is changed from 0.82 leading to 0.82 lagging and vice-versa. As shown in Fig. 14 and 15, the transient interval from one state to another is completed within one cycle.

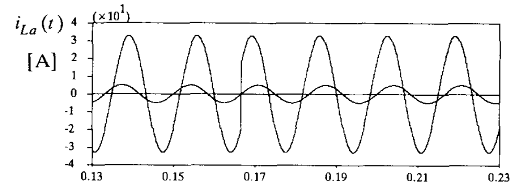

(a) load current

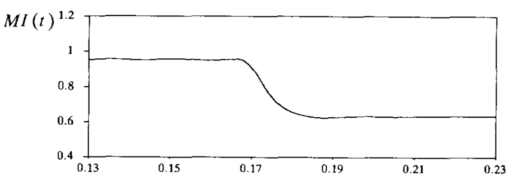

(b) modulation index(MI)

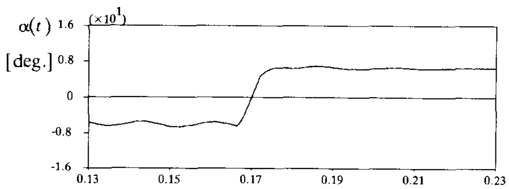

(c) phase angle(α)

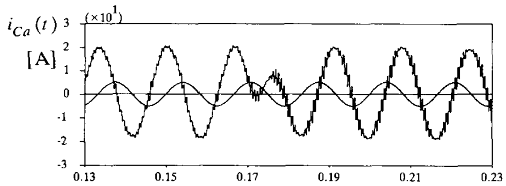

(d) compensator current

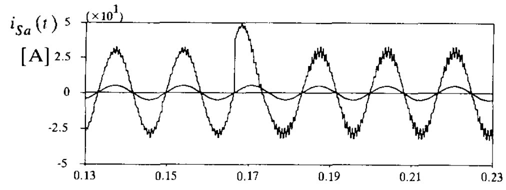

(e) source current

Fig. 14. step change of i_{La} from 0.82 lagging to 0.82 leading

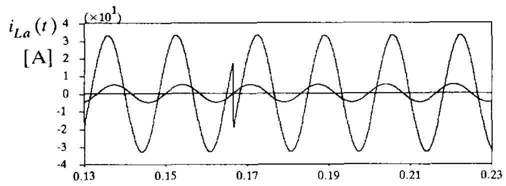

(a) load current

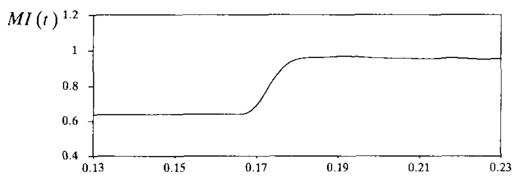

(b) modulation index(MI)

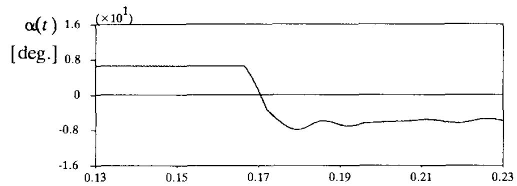

(c) phase angle(α)

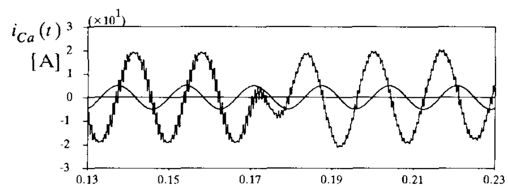

(d) compensator current

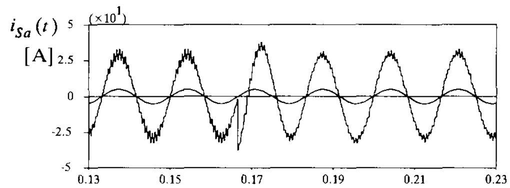

(e) source current

Fig. 15. step change of i_{La} from 0.82 leading to 0.82 lagging

VII. CONCLUSION

In this paper, a new static var compensator(SVC) using three-level inverter is proposed for high voltage and high power applications. The general and simple model for the proposed SVC is obtained and analyzed. Using the model, a new control method which controls the phase angle and modulation index simultaneously in the switching pattern is suggested to achieve fast response of SVC system without using additional voltage source. The validity of the modeling, analysis and control method of the proposed SVC system is proved by the computor simulation.

REFERENCE

[1] L. Gyugyi, "*Reactive Power Generation and control by thyristor circuits*" IEEE Trans. Ind. Appl., vol. IA-15, no. 5, pp. 521-532, Sept./Oct. 1979.

[2] Y. Sumi, T. Hasegawa, M. Ikeda and T. Matsura, "*New Static Var Control using Force-commutated Inverters*", IEEE Trans. Power App. Syst., vol. PAS-100, pp. 4216-4223, Sept. 1981.

[3] Luis T. Moran, Phoivos D. Ziogas, Geza Joos, "*Analysis and Design of a Three-Phase Synchronous Solid-State Var*", IEEE Trans. on Ind. Appl., vol.25, no.4, pp. 598-608, Jul./Aug. 1989.

[4] Luis T. Moran, Phoivos D. Ziogas, Geza Joos, "*Analysis and Design of a Three-Phase Current Source Solid-State Var*", IEEE Trans. on Ind. Appl., vol.25, no.2, pp. 356-365, Mar./Apr. 1989.

[5] Luis T. Moran, Phoivos D. Ziogas, Geza Joos, "*Analysis and Design of a Novel Three-Phase Solid-State Var*", IEEE Trans. on Ind. Appl., vol.25, no.4, pp. 609-619, Jul./Aug. 1989.

[6] Geza Joos, Luis T. Moran, Phoivos D. Ziogas, "*Performance Analysis of PWM Inverter VAR Compensators*", IEEE Trans. on Power Electronics, vol.6, no.7, pp. 380-391, July 1991.

[7] Akira Nabae, Isao Takahashi, Hirofumi Akagi, "*A New Neutral-Point-Clamped PWM Inverter*", IEEE Trans. on Ind. Appl., vol.1A-17, no.5, pp. 518-523, Sept./Oct. 1981.

[8] C. T. Rim, "*Analysis of Linear Switching Systems using Circuit Transformations*", 1990, KAIST